Tuning Bandwidths for Near-Threshold Stimuli in Area MT

KENNETH H. BRITTEN[1] AND WILLIAM T. NEWSOME[2]
[1]*University of California, Davis Center for Neuroscience and Section of Neurobiology, Physiology and Behavior, Davis, 95616; and* [2]*Howard Hughes Medical Institute and Department of Neurobiology, Stanford University School of Medicine, Stanford, California 94305*

Britten, Kenneth H. and William T. Newsome. Tuning bandwidths for near-threshold stimuli in area MT. *J. Neurophysiol.* 80: 762–770, 1998. It is not known whether psychophysical performance depends primarily on small numbers of neurons optimally tuned to specific visual stimuli, or on larger populations of neurons that vary widely in their properties. Tuning bandwidths of single cells can provide important insight into this issue, yet most bandwidth measurements have been made using suprathreshold visual stimuli, whereas psychophysical measurements are frequently obtained near threshold. We therefore examined the directional tuning of cells in the middle temporal area (MT, or V5) using perithreshold, stochastic motion stimuli that we have employed extensively in combined psychophysical and physiological studies. The strength of the motion signal (coherence) in these displays can be varied independently of its direction. For each MT neuron, we characterized the directional bandwidth by fitting Gaussian functions to directional tuning data obtained at each of several motion coherences. Directional bandwidth increased modestly as the coherence of the stimulus was reduced. We then assessed the ability of MT neurons to discriminate opposed directions of motion along six equally spaced axes of motion spanning 180°. A signal detection analysis yielded neurometric functions for each axis of motion, from which neural thresholds could be extracted. Neural thresholds remained surprisingly low as the axis of motion diverged from the neuron's preferred-null axis, forming a plateau of high to medium sensitivity that extended ~45° on either side of the preferred-null axis. We conclude that directional tuning remains broad in MT when motion signals are reduced to near-threshold values. Thus directional information is widely distributed in MT, even near the limits of psychophysical performance. These observations support models in which relatively large numbers of signals are pooled to inform psychophysical decisions.

INTRODUCTION

Two contrasting ideas have dominated inquiry concerning the relationship between perception and the activity of sensory neurons in the CNS. According to Horace Barlow's classic single neuron doctrine (Barlow 1972, 1995), a cortical neuron is tuned along a number of stimulus dimensions so that only a small, highly specific set of stimuli can excite the cell optimally. Furthermore, the optimal stimulus for each neuron is likely to differ given the large number of stimulus dimensions along which neurons can be tuned. From this point of view, each individual neuron acts as a highly specific detector (''cardinal cell'') for its optimal stimulus and thus wields substantial signaling power concerning the presence of this stimulus in the visual environment. According to this view, simple perceptual judgments would ideally be based on activity in a very small number of cortical neurons best tuned to the stimulus at hand. A key advantage of such ''sparse coding'' models is that they increase the efficiency of the representation by reducing statistical dependence among individual elements.

In an alternate coding strategy, a given stimulus excites a widely distributed population of neurons, and perceptual performance is guided by information contained in the entire population response. The signaling properties of individual neurons overlap substantially, and such redundancy in the distributed population provides insulation against central sources of noise, increases computational speed, and ensures robust performance in the face of neuronal loss. In such ''coarse coding'' models, even simple perceptual judgments are likely to depend on broadly distributed patterns of neural activity. Of course, these two coding strategies are not mutually exclusive; intermediate forms are possible. Also, it is possible that each is in use in different parts of the nervous system.

One key piece of evidence commonly used in support of coarse coding models lies in the apparently broad tuning of single cortical neurons along most stimulus dimensions, such as wavelength, spatial frequency, or movement direction. Such breadth of tuning leads to substantial redundancy between individual elements, consistent with the notion of coarse coding. However, these tuning measurements have typically been made at high stimulus strengths. There is no doubt that under such conditions (e.g., 100% contrast or fully coherent motion), there is a vast surplus of information available in central representations. Numerous distinct strategies of information coding or extraction could all be consistent with the high levels of performance measured under such conditions. Near threshold, however, this need not be the case; the statistics of the representation could be quite different. To address this problem, we measured tuning to stimuli of near-threshold intensities. Specifically, we sought to determine whether the directional bandwidth of cortical cells near behavioral threshold is different from the broad tuning typically observed at high stimulus strengths.

In this paper, we report such an analysis for directionally selective neurons in the middle temporal visual area (MT) of the macaque monkey, an extrastriate visual area that is involved in the analysis of visual motion (Albright 1984; Britten et al. 1992; Maunsell and Van Essen 1983a; Newsome and Paré 1988; Orban et al. 1995; Pasternak and Merigan 1994; Salzman et al. 1992; Schiller 1993; Schiller and Lee 1994; Zeki 1974). We measured the directional tuning of MT neurons for both near-threshold and suprathreshold stimuli. Our visual stimuli were stochastic random dot patterns in which we could vary the signal-to-noise ratio of the directional motion signal. Using these stimuli, we found that

0022-3077/98 $5.00

directional tuning of MT cells remains broad even near behavioral threshold. In addition, neuronal thresholds for signaling direction remained fairly low even for stimuli quite far removed from their preferred directions. These observations suggest that information remains broadly distributed across a cortical map, even near threshold, consistent with the notions of coarse coding. Considered together with our prior experimental and modeling studies (Britten et al. 1992, 1996; Shadlen et al. 1996), the present data suggest that directional judgments under our experimental regime are influenced by a population of MT neurons having a wide range of preferred directions.

METHODS

These data were obtained from area MT of two adult, female rhesus monkeys (*Macaca mulatta*). The general methods are similar to those used in previous studies and will be described only briefly. Before recording, each monkey was equipped with a head post for restraint, a scleral search coil to monitor eye position, and a recording cylinder implanted over the occipital cortex to allow microelectrode access to area MT from a posterior direction, 20° above horizontal in a parasagittal plane. This equipment was secured to the skull using a dental acrylic implant, and this procedure was performed under deep surgical anesthesia. The monkeys were given at least 2 wk to recover from surgery before recording. For recording experiments, the monkeys were removed from their home cages and seated in a primate chair in front of the cathode ray tube (CRT) screen on which the stimuli were displayed. They were required to fixate within 0.75–1.2° of a small spot projected on the screen; no discrimination was required. Successfully completed fixation trials were rewarded with a drop of water or juice; broken fixations were followed by a brief time-out period. All procedures complied with the National Institutes of Health and United States Department of Agriculture guidelines for the care and use of laboratory animals and had been approved by the Stanford University Animal Care and Use Committee.

Guide tubes for recording were secured inside the cylinder using a removable nylon grid with holes 1 mm apart (Crist et al. 1988) and were inserted through the dura using local anesthetic if necessary. On recording days, parylene-coated tungsten microelectrodes (Micro Probe) were introduced through the guide tube, and neural signals from these were amplified, filtered, and displayed using standard methods. Spikes were isolated using a time-amplitude window discriminator (Bak Electronics) and were fed as transistor-transistor logic pulses to the computer controlling the experiment. The electrode was advanced until a single-unit signal could be isolated, and appropriately moving dot patterns or moving bars were used as search stimuli. Once a single unit was isolated, the receptive field was mapped using hand-held stimuli, typically moving bars of light. Random dot stimuli were restricted to the classical receptive field (RF) in subsequent experiments.

Visual stimuli

The computer presented, via a fast D/A converter, streams of dots on the face of a vector display CRT (Xytron A21, P4 phosphor). These dots could either be replotted randomly on each iteration, or with a specified spatiotemporal offset, which determined the direction and speed of the apparent motion signal. In practice, the temporal interval between replottings of the signal dots was held fixed at 45 ms, and the speed of motion was varied by adjusting the spatial interval. The proportion of dots replotted in this way was determined by a parameter we term the *coherence* of the display. This parameter controlled the signal-to-noise ratio of the display and thus the salience of the motion. The coherence corresponds approximately linearly to total motion energy in the specified direction (Britten et al. 1993) and is independent of the average luminance as well as the specified motion parameters. The display was stochastic; the replotting of each dot was independent of all others and of its own history. Accordingly, the directional signal was randomly distributed both in space and in time, varying around a uniform mean. Each stimulus was 1 s in duration, and dots were presented at a rate of 6.67 kHz. The average luminance of the stimulus was 0.67 cd/M^2, and the contrast of each dot was very nearly 100% (background of 0.01 cd/M^2).

Stimuli were presented in blocks, varying both in coherence and in direction. Typically, stimuli were presented at three to five coherence levels at 30° intervals across one side of a neuron's direction tuning curve. The coherence levels were chosen to range from 100% down to a coherence level where the cell was minimally directional. The minimum coherence level was 12.8 or 25.6% for most cells; a smaller number were sampled down to 3.2 or 6.4%. If time permitted, data were collected from the other side of the tuning curve in a subsequent block. Within each block, stimuli were pseudorandomly interleaved, and a minimum data set consisted of 10 trials per condition. More blocks were run if time permitted.

Data analysis

Data were stored digitally as times of spike arrivals (1 ms resolution), and these were converted to spike counts by integrating over the entire 1-s stimulus period. Two different analyses were performed on these data. First, we performed bandwidth analysis to characterize the breadth of directional tuning of our cells as a function of coherence. For this purpose, the response-versus-direction data were fit with Gaussian functions of the form

$$\text{Response} = A\left[\frac{\exp(x-\mu)^2}{\sigma^2}\right] + B \qquad (1)$$

where A is response amplitude (i.e., dynamic range), μ specifies the center of the function, σ the bandwidth, and B is the baseline response at directions far from preferred (this need not be equal to the maintained activity, because of inhibition in the null direction). The present analysis focuses on the bandwidth parameter, σ; we have previously characterized the amplitudes of response in preferred and null direction (approximated by the parameters A and B) as a function of coherence (Britten et al. 1993).

In addition, threshold analysis similar to that previously employed in this laboratory was used to measure *sensitivity* as a function of direction for each cell. This analysis required complete data spanning 360° of direction, which was available on a subset of 43 cells. The goal of this analysis was to measure a *threshold* coherence level for each axis of motion along which the cell's responses were measured. This threshold estimates the performance of an ideal observer who deduces which of the two directions along the axis the dots were moving, given the information in the firing rate of the cell. The method [receiver operating characteristic (ROC) analysis] is derived from signal detection theory and has been applied in numerous neurophysiological studies (Bradley et al. 1987; Britten et al. 1992; Tolhurst et al. 1983; Vogels and Orban 1990). For each cell, axis of motion, and coherence level, we measured the discriminative capability of the cell using ROC analysis (Green and Swets 1966). The area under a ROC curve forms an unbiased, distribution-free estimator of the capability of the cell to discriminate between the two opposite directions along a given axis of motion. For each cell and axis, ROC area was plotted as a function of stimulus coherence to form a neurometric function relating performance to stimulus strength. We fitted each of these with a Quick function (Quick 1974) of the form

$$p = 1 - 0.5 \{\exp [-(c/\alpha)^{\beta}]\} \quad (2)$$

where P is the probability of a correct decision by the ideal observer, c is the coherence of the stimulus, α is the threshold (82% correct point), and β is a unitless parameter characterizing the steepness of the relationship. In previous work (Britten et al. 1992), we established that this function is a good description of neurometric data from MT cells' responses measured along the preferred-null axis. Note that in *Eq. 2*, the asymptotic performance is assumed to be unity; this assumption is similar to the one we have tested previously for optimal stimuli (Britten et al. 1992). We maintained this assumption in the present analysis even though nonoptimal axes of motion frequently yielded imperfect performance at the highest coherence level (ROC area < 1.0). We adopted this procedure so that neural thresholds measured along the various axes could be fairly and quantitatively compared. Allowing the asymptote to vary as a free parameter would preclude such a comparison because the threshold parameter is defined *relative to* the asymptote. We emphasize that the thresholds reported in this study reflect the same absolute level of neuronal performance (i.e., 82% correct) irrespective of the axis of motion.

For both types of fit, we evaluated the reliability of the best-fit function by comparing the quality of the fit to that of the mean response alone (Hoel et al. 1971). The log likelihood for each fit (which is distributed approximately as χ^2) was calculated both for the fit with more parameters (2 for the Quick function and 4 for the Gaussian), and also for the fit to the mean alone. The difference of these log likelihoods is also distributed approximately as χ^2, and the associated degrees of freedom is the difference in the number of free parameters in each fit. This statistic tests the null hypothesis that there is no significant improvement in fit by the full function. Conditions for which the null hypothesis could be rejected ($P < 0.05$) were retained for quantitative analysis. Inspection of the fits ''by eye'' suggested that this test was fairly stringent, and all of the retained fits were of high quality. For both types of fit, there was no indication that the fit parameters in the unreliable cases were biased.

Histology

During recording, cells were identified as being within MT according to reliable physiological landmarks, including *1*) consistently directional responses, *2*) reasonable RF size, with the diameter being approximately equal to the eccentricity, *3*) appropriate depth from the opercular surface, *4*) systematic progressions in preferred direction (Albright 1984), and *5*) shifts of RF location with electrode movement corresponding to the expected retinotopy of MT. After the experiments, the monkeys were anesthetized with ketamine hydrochloride, killed with an overdose of pentobarbital sodium, then perfused with normal saline followed by a 10% Formalin fixative solution. The brains were removed, blocked, and postfixed in 10% Formalin containing 30% sucrose. After equilibrating in sucrose, they were sectioned at 40 μm thickness on a horizontal freezing microtome. Alternate series of sections at 0.5-mm intervals were stained for Nissl substance and myelin (Gallyas 1979). MT was easily identified as a myelin-dense region on the posterior bank of the superior temporal sulcus (Allman and Kaas 1971; Ungerleider and Mishkin 1979; Van Essen et al. 1981). In both cases, the interval between recording and histological reconstruction prevented the use of marking lesions, but the overall region of intensive recording was easily visible from guide tube damage posterior to area MT. In both cases, this area corresponded well to the myeloarchitectonic boundaries of area MT.

RESULTS

These results were obtained from 52 cells in 2 monkeys. Data from two representative MT neurons are shown in Fig. 1. The neuron shown in *A* and *B* is broadly tuned for direction, whereas the neuron illustrated in *C* and *D* is more narrowly tuned. Figure 1, *A* and *C*, depicts firing rate as a function of direction for several coherence levels, and it is clear that the responses increase systematically as a function of coherence within the excitatory portion of each tuning curve. Figure 1, *B* and *D*, depicts the same data following normalization to the range of response in each tuning curve. The normalized tuning curves superimpose nicely. These example data illustrate two important points. First, the responses increase monotonically and approximately linearly as a function of coherence for every direction tested. This extends the observations of Britten et al. (1993) to stimulus directions other than the preferred and null. Second, the normalized plots on the *right* show that the shape of the direction tuning functions are not strongly influenced by the coherence of the stimulus. In Fig. 1*D*, there is a slight suggestion that the direction tuning functions become somewhat broader at lower coherence, because the dashed line curves tend to lie outside the solid line curve representing 100% coherence.

Bandwidth analysis

To parameterize the shape of the direction tuning functions and their dependence on the coherence of the stimulus, we fit each direction tuning curve with a Gaussian function (*Eq. 1*). Figure 2 illustrates Gaussian fits to data from two coherence levels. The mean $\pm$ SD ($\pm 1\ \sigma$) of the two Gaussians, indicated by the vertical lines, are in good agreement for the two functions despite the substantial difference in the amplitudes. Thus the two functions are largely scaled replicas of each other.

Figure 3 illustrates bandwidth as a function of stimulus coherence for our entire sample of 52 cells from two monkeys. We included data only from tuning functions that passed our goodness-of-fit criterion (see METHODS), and the bandwidth values are thus quite reliable. Screening the data according to the goodness-of-fit criterion reduced the number of data points from low coherence values because few of these curves were better fit by a Gaussian than by the mean alone. The simple regression relating bandwidth to coherence is indicated by the approximately horizontal line in the figure, which had an intercept of 90.9 and a slope of -0.131. This relationship was not significant ($P = 0.17$), although there is a weak trend toward larger bandwidths at lower coherence values. This effect, if real, is clearly modest in magnitude, because it predicts only a 14% change in bandwidth across the range of 0–100% coherence.

This population analysis, however, might miss effects in individual cells because it pools data across the entire sample of neurons. The flat regression line in Fig. 3 would be misleading, for example, if one-half the cells had a strong positive slope in the relationship between bandwidth and coherence whereas the others had an equally strong negative slope. We therefore repeated the regression analysis, estimating a regression slope for each cell individually. Figure 4 illustrates the distribution of slopes obtained from this analysis. This mean of the distribution is -0.21, again suggesting a modest negative relationship between bandwidth and coherence. The mean of this distribution is significantly <0 (2-

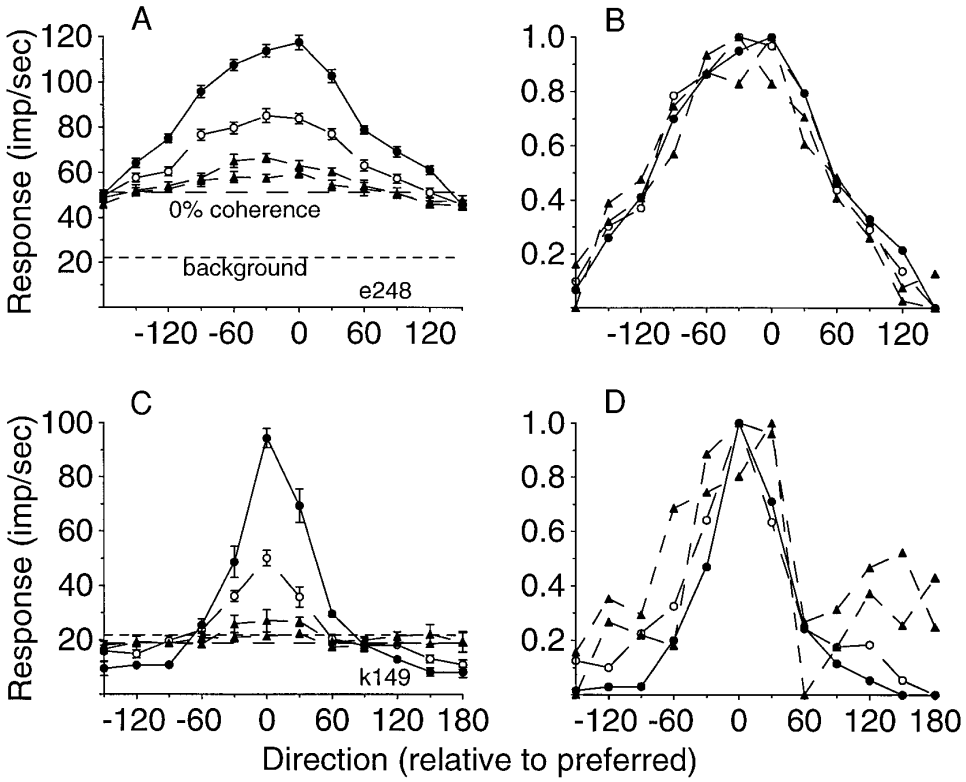

FIG. 1. Direction tuning functions for 2 middle temporal area (MT) neurons measured at different motion coherences. *A* and *B*: results for a broadly tuned cell. *C* and *D*: corresponding results for a more narrowly tuned cell. The coherence levels represented in all panels are 12.8, 25.6, 51.2, and 100% (bottom to top in *A;* symbols and line types match for all panels). *A* and *C*: average responses over the 1-s stimulus period, and the bars represent standard errors. *B* and *D*: same response functions, individually normalized to unit amplitude and zero baseline.

tailed $t = 2.18$, $P = 0.034$). Thus, analyzed on a per cell basis, the weak relationship seen in Fig. 3 becomes statistically significant. This is only evident after pooling; in only 2/52 cases was the *individual* correlation significant ($P < 0.05$), because the number of coherence values contributing to each was small. As seen previously, the relationship is not strong, predicting only modest changes in bandwidth across the full range of possible stimulus strengths. Because of the uncertainty in the individual slope estimates, the resulting mean slope should be interpreted with caution.

This bandwidth analysis assumes that the Gaussian functions were equally valid descriptions of the cells' response functions at all stimulus strengths. Although reasonable, this assumption may be confirmed rigorously by analysis of the residuals of the best-fit functions. In Fig. 5, we show the average residuals for each stimulus strength for which we had a sample size of over three cases at each direction. The residuals for each cell's fit were scaled to the amplitude parameter of the Gaussian, and a running 15-point boxcar average was computed. The curves are vertically offset from

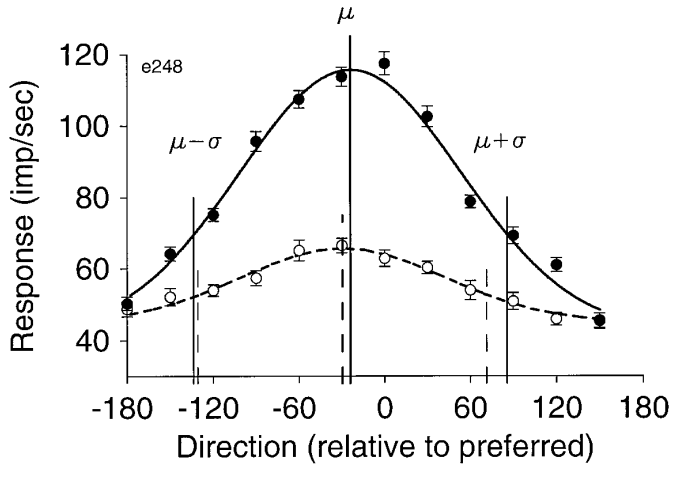

FIG. 2. Example of the bandwidth analysis. For a single cell we plot the response as a function of direction for 2 coherence values. ●, data for 100% coherence stimuli; ○, 25.6% coherence. For each set of data we fit the best Gaussian function (*Eq. 1*), which is shown by the corresponding curve. Solid and dashed vertical lines depict the mean ± 1σ points for the high and low coherence functions, respectively.

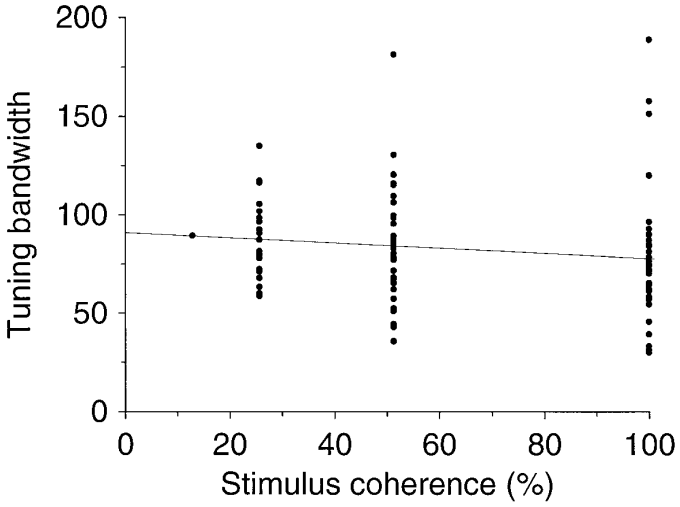

FIG. 3. Relationship between tuning bandwidth and stimulus coherence for all cells. A data set was included only if the fitted Gaussian function met a strict goodness of fit criterion (see METHODS). The line shows the simple regression relationship derived from the 95 data sets that passed this test.

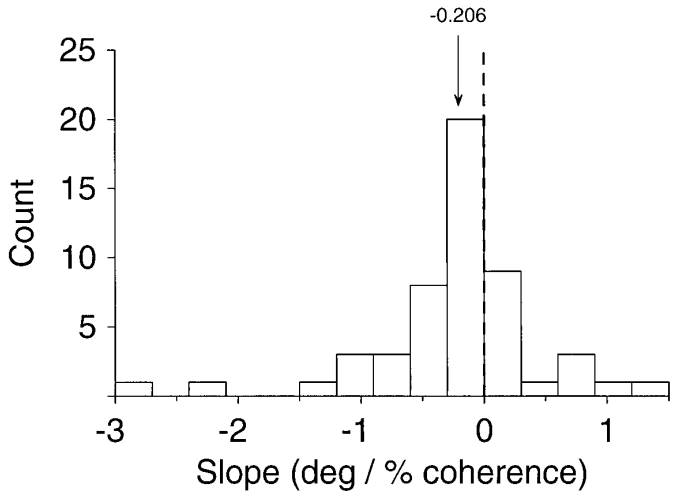

FIG. 4. Relationship between bandwidth and coherence, analyzed on a per-cell basis. For each cell, a simple regression was performed, and the slope value was taken from this relationship. The resulting slopes were compiled into the histogram, whether or not they were individually significant. The arithmetic mean of the slope values is indicated above the arrow.

each other for graphic clarity; each horizontal line corresponds to zero for the associated curve. The figure shows that the residuals do not systematically change for the weaker stimuli, although they become somewhat erratic for the lowest strength stimulus. The latter effect arises because fewer cases were run at low coherence and because the relative amplitude of the noise grows as the response shrinks. All of the curves appear nonsystematic in their fluctuations and converge on zero at higher coherences. These observations confirm the choice of a Gaussian function for describing these directional data and show in a more assumption-free manner that the functions do not change shape systematically with the coherence of the stimuli.

ROC analysis

We analyzed each neuron's ability to discriminate opposed directions of motion using the method of ROC analysis, in a manner similar to our previous work (for details, see Britten et al. 1992). This method extracts a performance estimate from the two distributions of spike counts obtained for the two opposed directions of motion along a particular axis. If these distributions are similar, the performance estimate (ROC area) will be close to chance (0.5, or 50% correct). If the response distributions are nonoverlapping; however, the performance estimate will be perfect (1.0, or 100% correct). In effect, the ROC area estimates the performance of an ideal observer who is trying to deduce the stimulus from the spike rate of the cell. For 43 neurons with adequate data sets (data collected for all 6 axes of motion), we computed ROC areas for each axis of motion and coherence level tested. The contour plot in Fig. 6 illustrates average neuronal performance (ROC area) as a function of axis of motion and coherence level. The preferred direction was defined as the peak of the Gaussian fit to the data at the highest coherence used.

We emphasize that Fig. 6 contains *all* available data for these 43 neurons; no screening for goodness-of-fit was employed because these data are not derived from fitted neurometric functions. Thus Fig. 6 reflects the behavior of this population of neurons faithfully, incorporating even conditions in which the neuron may have little or no discriminative power (i.e., an axis of motion nearly orthogonal to the preferred-null axis).

The contours in Fig. 6 are quite shallow in the central 30–40°, indicating the presence of a broad region of high sensitivity (low threshold). Thus the discriminative capacity of these MT neurons is not tightly restricted to the preferred-null axis of motion. The contours do not rise steeply until ~60° away from the preferred-null axis. We conclude that directional information of potential use for threshold psychophysical discriminations is broadly distributed across the map of direction in MT.

As we and others have shown previously, the performance (or sensitivity) of an individual neuron can be characterized by compiling a ''neurometric function'' that plots ROC area as a function of coherence. Neuronal thresholds are derived from sigmoidal curves fitted to these data, where threshold is considered to be the coherence value that would support a criterion level of performance (82% correct) by an ideal observer of the neuron's responses (the 82% correct level is shown for the averaged data by the bold contour in Fig. 6). For each neuron in our sample, we estimated performance by computing such neurometric functions separately for each axis of motion tested. Figure 7 shows how these estimated threshold values vary as a function of the directional axis for the two example cells shown in Fig. 1. In each case, 0° refers to the preferred-null axis. The open symbols at the ends of both of these functions denote points where the fit neurometric functions failed our goodness-of-fit test (see METHODS) and should be considered unreliable estimates.

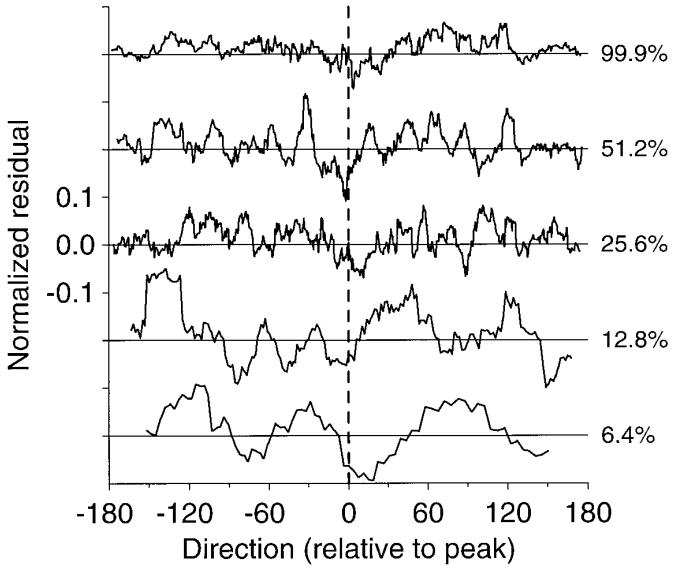

FIG. 5. Residuals from the Gaussian fits. For each coherence employed between 6.4 and 100%, we plot the average (across cells), normalized residual as a function of direction. Data were aligned to the peak of the best-fit Gaussian, and a running 15-point arithmetic mean was computed for each coherence (solid curves). All individual residuals were scaled to the amplitude parameter for the Gaussian fit for that cell and coherence value before averaging; this gives all observations equal weight despite differences in firing rate or dynamic range. The curves were offset from each other vertically for graphic clarity.

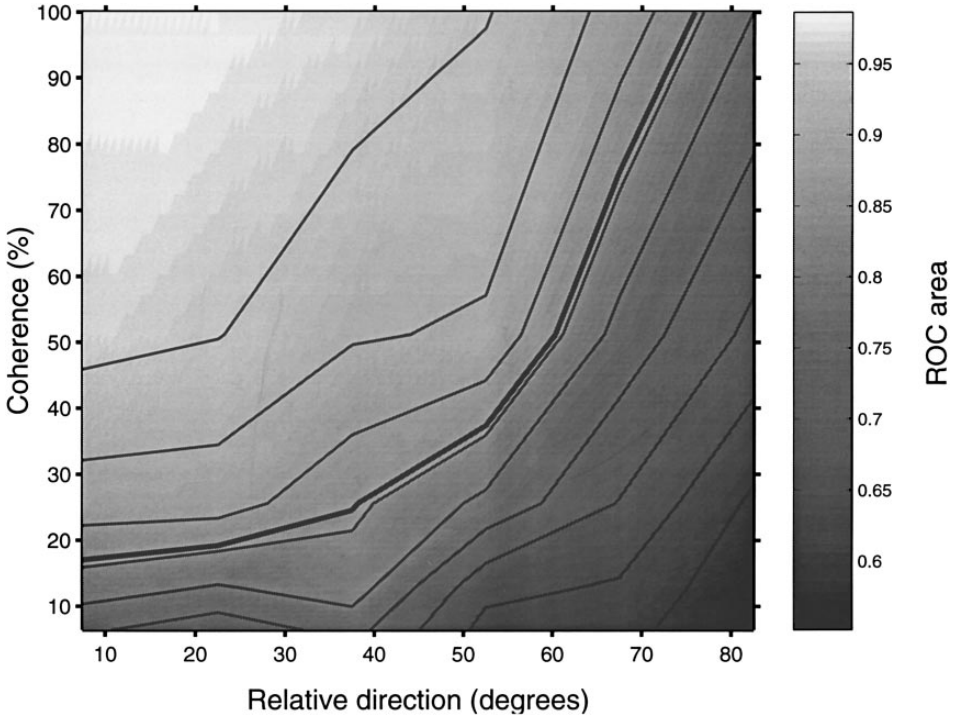

FIG. 6. Average performance of 43 MT cells, calculated using receiver operating characteristic analysis, as a function of coherence and direction of the stimuli. The gray level and the contours both depict the average ROC estimate of performance, and the bold contour shows performance of 82% correct, a value we have defined as threshold performance. Directional data were binned for averaging in 15° bins, and all coherences between 6.4 and 100% were included. As indicated by the calibration bar to the right, lighter gray values correspond to better performance (ROC areas nearer to 1.0).

The rising threshold on both sides of these functions tell us that the neurons' sensitivities decrease with increasing angle from the preferred-null axis. The breadth of the threshold functions plotted here correspond fairly well to the width of the tuning functions presented in Fig. 1. The broadly tuned cell (Fig. 7*A* and Fig. 1, *A* and *B*) has a region of low thresholds that spans three directional axes, or 60°, whereas the more narrowly tuned cell had a narrower region of low thresholds ~30° in width. Note also that the rather subtle asymmetries in the tuning functions presented in Fig. 1 produce more striking asymmetries in the threshold functions in Fig. 7.

Figure 8 illustrates the derived thresholds for the 43 cells in our sample for which we gathered adequate data to perform this analysis. The filled circles illustrate statistically reliable threshold measurements, according to our goodness-of-fit criterion (see METHODS), and the solid line is a running nine-point geometric mean of the reliable points. The small points depict threshold estimates from functions that failed our goodness-of-fit test and should be considered unreliable; the small Xs indicate such points that went off-scale vertically. This figure reveals a broad trough of low thresholds, as one would expect from the raw ROC data in Fig. 6. Thus individual cell thresholds, like the population average performance, double ~50–60° from the preferred direction. These two portrayals differ somewhat at more distant angles, reflecting the fact that we cannot accurately estimate thresholds when the stimuli become grossly nonoptimal. The number of high, unreliable threshold estimates (Xs) increases substantially at nearly orthogonal angles; these unreliable values are *not* included in the running mean in Fig. 8, although the actual ROC measurements *do* contribute to the portrayal in Fig. 6. Both analyses agree, however, that for most MT neurons a broad region of high sensitivity extends well away from the preferred-null axis of motion.

DISCUSSION

The results of this study confirm and extend numerous studies of tuning properties of MT neurons (Albright 1984; Lagae et al. 1993; Maunsell and Van Essen 1983b; Snowden et al. 1992). We find broad tuning for direction, both with high and low coherence stimuli. Bandwidths became significantly broader at low coherences, but this effect was small. Additionally, analysis of neuronal discrimination thresholds showed that MT neurons maintained differential sensitivity to opposed directions for axes of motion quite far removed from the preferred-null axis. Thus large numbers of neurons carry signals appropriate for performing the task, even near psychophysical threshold. This pattern of results appears consistent with coarse coding models of the representation of stimulus direction in MT.

Relationship with previous work

This result may be compared with measurements made using other classes of stimuli in other cortical areas. In primary visual cortex of cats, tuning bandwidths for orientation and spatial frequency are largely invariant with stimulus contrast (Albrecht et al. 1984; Sclar and Freeman 1982). This comparison is particularly interesting because contrast-response functions frequently saturate, whereas coherence-response functions rarely do (Britten et al. 1993). Contrast saturation might be expected to change the shape of tuning functions, because it would broaden the top of these functions, as the high rates near the center of the function reach the saturating response. The modest effects of coherence on bandwidth in our results are unexpected on these grounds, because coherence-response functions are linear on average. However, these effects are small, affecting bandwidth by 15–30% at most, and the general finding appears to be that

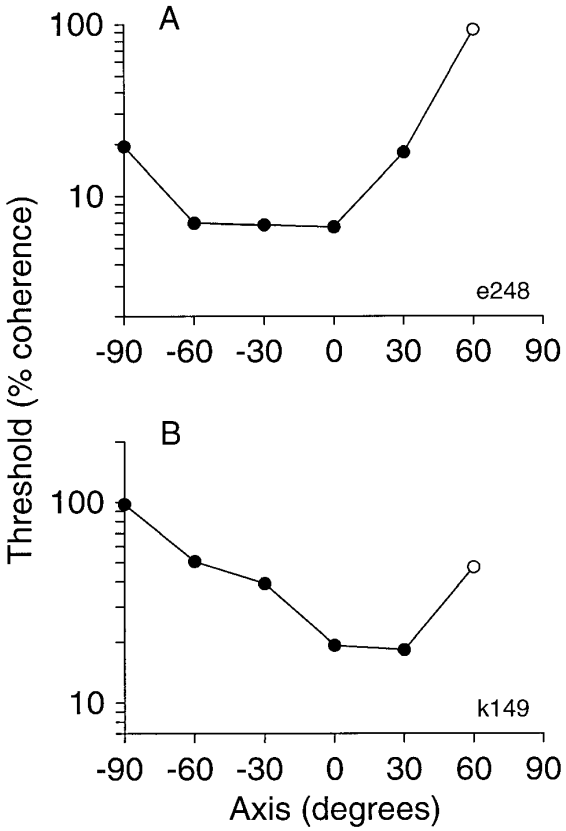

FIG. 7. Neurometric thresholds plotted as a function of axis of motion for the same cells illustrated in Fig. 1. The axis of motion is given in degrees of polar angle relative to the preferred-null axis. Along each axis, data from opposed directions were used to calculate a neurometric function from which neural thresholds were derived. ○, statistically unreliable threshold estimates (see METHODS).

tuning functions are largely invariant with changes in stimulus strength. This, of course, is highly desirable from a theoretical point of view, because it stabilizes the representation of image features against changes in viewing conditions or the addition of noise.

The present results have particularly important implications for previous analyses from this laboratory concerning the neural processing mechanisms that underlie psychophysical performance on a specific direction discrimination task (Britten et al. 1992, 1996; Newsome and Paré 1988; Shadlen et al. 1996). The task involved discrimination of opposed directions of motion using the same family of stochastic motion stimuli employed in the current study. We now consider the import of the current results for models of how directional signals in MT mediate performance on this task. The relevance of the current results for other motion discrimination tasks is less clear (e.g., Orban et al. 1995; Pasternak and Merigan 1994; Snowden et al. 1992), and we therefore have little to say about them.

One limitation of our previous experiments was the choice to measure thresholds of neurons with the stimulus parameters (size, direction, speed) *optimized* for each neuron. From a population coding perspective, this means the measurements were made only on neurons that were likely to be very sensitive to the motion signals in the stimuli. Our main finding was that MT neurons assessed in this way were remarkably sensitive; their thresholds generally approximated the monkey's psychophysical thresholds made on the same set of trials (Britten et al. 1992). Initially, this led us to suggest that perhaps very small numbers of MT neurons were involved in any particular task configuration (Newsome et al. 1989). However, consideration of two other measurements [shared noise between neurons and the correlation of neuronal discharge with choice (Britten et al. 1996; Zohary et al. 1992)] subsequently led us to favor models in which much larger pools of neurons are involved in such a direction discrimination task. Simulations showed that larger pools can produce behavioral thresholds consistent with those we observed, even if the pools include additional neurons whose sensitivity to direction is an order of magnitude worse than those we actually measured. Our simulations suggest, in fact, that such insensitive neurons *must* be included in the sensory pool to reconcile the complete set of physiological and psychophysical data (Shadlen et al. 1996). In our computational analysis, we simulated these ''insensitive'' neurons by an arbitrary linear scale factor because we had never measured the responses of nonoptimally tuned neurons. The present measurements allow us to ground this modeling work in the actual responses of nonoptimally tuned neurons in MT.

The most successful version of a ''pooling model'' consistent with our physiological and psychophysical data used pools of MT neurons whose average neuronal threshold was 2.5 times higher than the average threshold measured under optimal conditions. The data in Fig. 8 enable us to estimate what fraction of the directional map must be included to achieve an average neuronal threshold that is 2.5 times

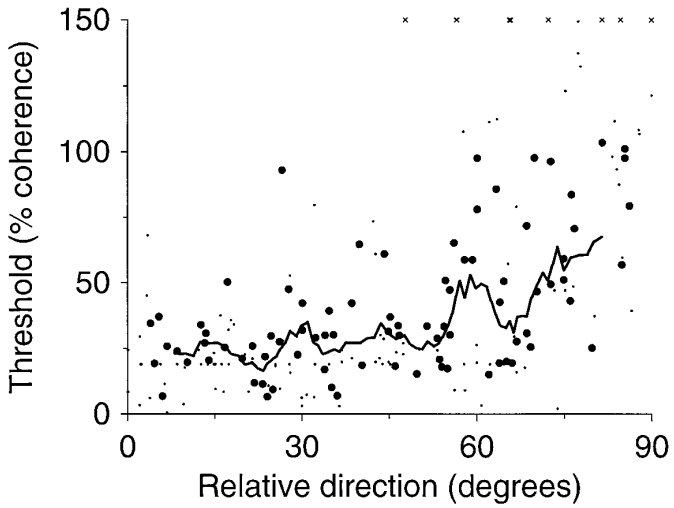

FIG. 8. Neurometric thresholds as a function of axis of motion for all cells for which sufficient data were obtained. The axis of motion is given in degrees relative to the preferred direction, defined as the peak of the Gaussian function fit to the highest coherence stimulus. Large circles indicate statistically reliable threshold measurements; small circles represent cases that failed our goodness of fit test (see METHODS). Thirty-four extreme values have been removed from this latter group. Solid curve corresponds to a running 9-point boxcar geometric mean of only the reliable threshold estimates. These data are subject to 2 sources of noise not present in previous work from this laboratory (Britten et al. 1992): smaller number of trials per coherence and smaller number of coherence levels presented. Both were necessary compromises because of the number of directions presented, but neither should in principle be a source of bias.

greater than the optimal thresholds measured along the preferred-null axis. For each nonpreferred axis of motion tested for each cell, we computed the ratio of neuronal threshold off-axis to neuronal threshold along the preferred-null axis. Interestingly, the geometric mean of this ratio across the sample of well-estimated thresholds was 2.71, which is remarkably similar to the value of 2.5 derived independently from the simulations. The similarity of these ratios raises the possibility that most neurons with receptive fields at a particular location in space, irrespective of their preferred directions, contribute to psychophysical decisions about stimuli at that location (assuming that the relationship between neuronal threshold and axis of motion in Fig. 8 is representative of most MT neurons). According to the logic of our opponent model (Britten et al. 1992; Shadlen et al. 1996), the neurons would be formed into two broad pools, each one centered around one of the two opposed directions of motion in a particular discrimination between opposed alternatives.

The data in this study, of course, permit us to estimate the effects on neuronal threshold of a single manipulation only, making stimuli nonoptimal by changing the axis of motion. The usefulness of a neuron for a given psychophysical discrimination must also be affected by variation in other stimulus parameters such as spatial location, but we have no quantitative measurements of these effects. Two related observations speak to this issue, however. First, the area-response functions of MT neurons typically rise quite steeply (Born and Tootell 1992; Raiguel et al. 1995), suggesting that a stimulus need not overlap the RF by much to generate a useful directional signal in the cell. Second, the RFs of MT neurons are large, with diameters roughly equal to their eccentricity (Maunsell and Van Essen 1983a; Zeki 1974). Together these observations suggest that the pool of available signals in MT is very large, and that a substantial fraction of MT neurons might carry signals useful for any given configuration of our task.

Stimulus effects

The manipulation of stimulus strength employed in the present work is complex because it changes the distribution of motion energy in the stimulus without changing the total energy in the stimulus (Britten et al. 1993). As coherence is reduced, a broad region of increased motion energy forms, including velocities near but not identical to the specified motion signal. Thus, at low coherence levels, the somewhat larger directional bandwidths we observe might result from changes in the stimulus itself, rather than changes in the neuronal representation per se. To explore this possibility, we have performed computer simulations similar to those we have reported in previous work (Britten et al. 1993). We designed motion-energy filters whose spatiotemporal characteristics resembled those of MT cells, and we simulated their responses to random dot stimuli like those in the present work. Across a wide range of model parameter values, direction tuning bandwidths were completely unaffected by the coherence of the stimuli. Thus we believe that the modest increase in bandwidth observed in our experiments arises from the biology of the system, rather than being a trivial consequence of the distribution of motion energy in our stimuli.

Coarse or sparse coding in MT?

The principal result of this work is that the distribution of information on the map of direction in MT is very broad, even for weak motion signals near psychophysical threshold. This appears to contrast with the predictions of sparse coding schemes. One way of visualizing these predictions is to picture a ''hill'' of activity on the map of direction in MT, and then to imagine how it changes as the stimulus is made weaker. If one imagines such a hill ''sinking'' past some threshold, then as performance limits are reached, only the very tip of the hill would be visible, and useful information would become highly localized within MT. Thus a representation that appeared coarsely coded at high stimulus intensities could be quite sparsely coded near threshold. A variety of nonlinearities in the pathway leading to MT could produce such effects. However, our results argue against such a picture: as the stimulus is made weaker, the hill simply scales down in height without changing its shape. If anything, the peak of activity becomes a little broader, not narrower. Thus the ideal observer charged with the job of extracting information from this representation would not change strategy for weaker stimuli.

Another argument raised in favor of sparse coding schemes derives from the multiple dimensions encoded by any single cortical area (e.g., Barlow and Tripathy 1997). Although MT appears more specialized than many cortical areas, it probably still represents at least six stimulus dimensions (2 dimensions of space, 2 of velocity, 1 of stereoscopic depth, and possibly orientation, spatial scale, and surround velocity as well). Thus the representation along any single dimension (such as direction of motion) can appear quite redundant, if the test stimuli were optimized along the other relevant dimensions. In our experiments, we attempted to optimize along only a subset of these stimulus dimensions (2 of space and 2 of velocity), yet the representation still appears coarsely coded and thus not highly ''efficient.'' As suggested by Barlow (Barlow and Tripathy 1997), this might reflect the advantage of averaging out noise in the image or its representation by pooling across inputs, each representing somewhat different values along some dimension. An inescapable consequence of such averaging is the broadening of tuning functions, and a concomitant decrease in the ''sparseness'' of the representation. Given that noise is most limiting near threshold, it would be advantageous to maintain a coarse code for such stimuli. By pooling broadly across available signals, one maintains sensitivity to the presence and rough identity of stimuli nearly lost in noise.

The authors thank J. Stein for expert technical assistance. We also thank M. N. Shadlen and B. A. Olshausen for helpful discussion.

This work was supported by National Eye Institute Grants EY-05603 to W. T. Newsome and EY-10562 to K. H. Britten. W. T. Newsome is an Investigator of the Howard Hughes Medical Institute.

Address for reprint requests: K. H. Britten, UC Davis Center for Neuroscience, 1544 Newton Ct., Davis, CA 95616.

Received 14 October 1997; accepted in final form 14 April 1998.

REFERENCES

ALBRECHT, D. G., FARRAR, S. B., AND HAMILTON, D. B. Spatial contrast adaptation characteristics of neurones recorded in the cat's visual cortex. *J. Physiol. (Lond.)* 347: 713–739, 1984.

ALBRIGHT, T. D. Direction and orientation selectivity of neurons in visual area MT of the macaque. *J. Neurophysiol.* 52: 1106–1130, 1984.

ALLMAN, J. M. AND KAAS, J. H. A representation of the visual field in the caudal third of the middle temporal gyrus of the owl monkey (*Aotus trivirgatus*). *Brain Res.* 31: 85–105, 1971.

BARLOW, H. Single units and sensation: a neuron doctrine for perceptual psychology? *Perception* 1: 371–394, 1972.

BARLOW, H. The neuron doctrine in perception. In: *The Cognitive Neurosciences,* edited by M. Gazzaniga. Cambridge, MA: MIT Press, 1995, p. 415–435.

BARLOW, H. AND TRIPATHY, S. P. Correspondence noise and signal pooling in the detection of coherent visual motion. *J. Neurosci.* 17: 7954–7966, 1997.

BORN, R. T. AND TOOTELL, R. B. Segregation of global and local motion processing in primate middle temporal visual area. *Nature* 357: 497–499, 1992.

BRADLEY, A., SKOTTUN, B. C., OHZAWA, I., SCLAR, G., AND FREEMAN, R. D. Visual orientation and spatial frequency discrimination: a comparison of single cells and behavior. *J. Neurophysiol.* 57: 755–772, 1987.

BRITTEN, K. H., NEWSOME, W. T., SHADLEN, M. N., CELEBRINI, S., AND MOVSHON, J. A. A relationship between behavioral choice and the visual responses of neurons in macaque MT. *Vis. Neurosci.* 13: 87–100, 1996.

BRITTEN, K. H., SHADLEN, M. N., NEWSOME, W. T., AND MOVSHON, J. A. The analysis of visual motion: a comparison of neuronal and psychophysical performance. *J. Neurosci.* 12: 4745–4765, 1992.

BRITTEN, K. H., SHADLEN, M. N., NEWSOME, W. T., AND MOVSHON, J. A. Responses of neurons in macaque MT to stochastic motion signals. *Vis. Neurosci.* 10: 1157–1169, 1993.

CRIST, C. F., YAMASAKI, D.S.G., KOMATSU, H., AND WURTZ, R. H. A grid system and a microsyringe for single cell recording. *J. Neurosci. Methods* 26: 117–122, 1988.

GALLYAS, F. Silver staining of myelin by means of physical development. *Neurol. Res.* 1: 203–209, 1979.

GREEN, D. M. AND SWETS, J. A. *Signal Detection Theory and Psychophysics.* New York: Wiley, 1966.

HOEL, P., PORT, S., AND STONE, C. *Introduction to Statistical Theory.* Boston, MA: Houghton Mifflin, 1971.

LAGAE, L., RAIGUEL, S., AND ORBAN, G. S. Speed and direction selectivity of macaque middle temporal neurons. *J. Neurophysiol.* 69: 19–39, 1993.

MAUNSELL, J.H.R. AND VAN ESSEN, D. C. Functional properties of neurons in the middle temporal visual area (MT) of the macaque monkey. I. Selectivity for stimulus direction, speed and orientation. *J. Neurophysiol.* 49: 1127–1147, 1983a.

MAUNSELL, J.H.R. AND VAN ESSEN, D. C. Functional properties of neurons in the middle temporal visual area (MT) of the macaque monkey. II. Binocular interactions and the sensitivity to binocular disparity. *J. Neurophysiol.* 49: 1148–1167, 1983b.

NEWSOME, W. T., BRITTEN, K. H., AND MOVSHON, J. A. Neuronal correlates of a perceptual decision. *Nature* 341: 52–54, 1989.

NEWSOME, W. T. AND PARÉ, E. B. A selective impairment of motion perception following lesions of the middle temporal visual area (MT). *J. Neurosci.* 8: 2201–2211, 1988.

ORBAN, G. A., SAUNDERS, R. C., AND VANDENBUSSCHE, E. Lesions of the superior temporal cortical motion areas impair speed discrimination in the macaque monkey. *Eur. J. Neurosci.* 7: 2261–2276, 1995.

PASTERNAK, T. AND MERIGAN, W. H. Motion perception following lesions of the superior temporal sulcus in the monkey. *Cerebr. Cortex* 4: 247–259, 1994.

QUICK, R. F. A vector magnitude model of contrast detection. *Kybernetik* 16: 65–67, 1974.

RAIGUEL, S., VAN HULLE, M. M., XIAO, D. K., MARCAR, V. L., AND ORBAN, G. A. Shape and spatial distribution of receptive fields and antagonistic motion surrounds in the middle temporal area (V5) of the macaque. *Eur. J. Neurosci.* 7: 2064–2082, 1995.

SALZMAN, C. D., MURASUGI, C. M., BRITTEN, K. H., AND NEWSOME, W. T. Microstimulation in visual area MT: effects on direction discrimination performance. *J. Neurosci.* 12: 2331–2355, 1992.

SCHILLER, P. The effects of V4 and middle temporal (MT) area lesions on visual performance in the rhesus monkey. *Vis. Neurosci.* 10: 717–746, 1993.

SCHILLER, P. H. AND LEE, K. The effect of lateral geniculate nucleus, area V4 and middle temporal (MT) lesions on visually guided eye movements. *Vis. Neurosci.* 11: 229–241, 1994.

SCLAR, G. AND FREEMAN, R. D. Orientation selectivity in the cat's visual cortex is largely invariant with stimulus contrast. *Exp. Brain Res.* 46: 457–461, 1982.

SHADLEN, M. N., BRITTEN, K. H., NEWSOME, W. T., AND MOVSHON, J. A. A computational analysis of the relationship between neuronal and behavioral responses to visual motion. *J. Neurosci.* 16: 1486–1510, 1996.

SNOWDEN, R. J., TREUE, S., AND ANDERSEN, R. A. The response of neurons in areas V1 and MT of the alert rhesus monkey to moving random dot patterns. *Exp. Brain Res.* 88: 389–400, 1992.

TOLHURST, D. J., MOVSHON, J. A., AND DEAN, A. F. The statistical reliability of signals in single neurons in cat and monkey visual cortex. *Vision Res.* 23: 775–785, 1983.

UNGERLEIDER, L. G. AND MISHKIN, M. The striate projection in the superior temporal sulcus of *Macaca mulatta*: location and topographic organization. *J. Comp. Neurol.* 188: 347–366, 1979.

VAN ESSEN, D. C., MAUNSELL, J.H.R., AND BIXBY, J. L. The middle temporal visual area in the macaque: myeloarchitecture, connections, functional properties and topographic representation. *J. Comp. Neurol.* 199: 293–326, 1981.

VOGELS, R. AND ORBAN, G. A. How well do response changes of striate neurons signal differences in orientation: a study in the discriminating monkey. *J. Neurosci.* 10: 3543–3558, 1990.

ZEKI, S. M. Functional organization of a visual area in the posterior bank of the superior temporal sulcus of the rhesus monkey. *J. Physiol. (Lond.)* 236: 549–573, 1974.

ZOHARY, E., SHADLEN, M. N., AND NEWSOME, W. T. Correlated neuronal discharge rate and its implications for psychophysical performance. *Nature* 370: 140–143, 1994.